



# Characteristics and consequences of lava dome collapse at Ruawahia, Taupo Volcanic Zone, New Zealand

P. A. Ashwell<sup>1</sup> · B. M. Kennedy<sup>1</sup> · M. Edwards<sup>2</sup> · J. W. Cole<sup>1</sup>

Received: 29 March 2017 / Accepted: 14 March 2018 / Published online: 4 April 2018  
© Springer-Verlag GmbH Germany, part of Springer Nature 2018

## Abstract

The eruption of large, rhyolitic lava domes may be accompanied by the formation of large block and ash flows. This may be linked to the style of dome extrusion—whether it forms a series of individual lobes, flows or spines (exogenous) or grows by internal inflation (endogenous). Lava domes can transition from one extrusive style to another as a result of a change in extrusion rate or the formation of facilitating structures such as shear zones. How this change can affect large rhyolitic lava domes is unclear as there are few historically recorded rhyolitic dome eruptions. Here, we present structures at Ruawahia lava dome (a well exposed ~700-year-old lava dome), how these facilitating structures enable exogenous extrusion at Ruawahia dome, and link this to collapse episodes along the fringes of the dome during growth. Ruawahia dome is part of the Tarawera dome complex, a chain of domes running parallel to regional structures across the Okataina caldera complex in the Taupo Volcanic Zone, New Zealand. Ruawahia dome consists of (1) a high porosity (44–52%), crystalline (65% DRE), locally brecciated carapace facies with rare bread-crusting and ‘ropey’ flow textures; (2) a core facies of dominantly low to moderate porosity (20–25%) with elongate vesicles that mark weak flow bands; and (3) thin (< 5 m thick) interior breccia zones. Flow bands at Ruawahia are complex and do not fit with hypothesised flow band orientations attributed to a single phase of exogenous or endogenous dome growth. Inward dipping flow bands on ramp structures on the flow surface suggest a flow-like (coulée) morphology; however, steeply dipping and multidirectional flow bands on the edges of the dome challenge this hypothesis. Widespread block and ash flow deposits have been sourced from the leading dome fronts to the NW and SE; these collapse events left behind inflated and bread-crusting outcrops on these dome fronts, suggesting syn-eruption collapse events that led to expansion of a hot, pressurised dome interior. We consider Ruawahia erupted from multiple, aligned vents, either as lobes confined within the crater of a pyroclastic cone formed during the initial Plinian phase of the eruption or those able to flow down the cone flank. The confined lobes formed steep internal breccia zones as individual dome lobes extruded past one another. Lobes that were able to overcome the pyroclastic cone rim (or where the vent was outside the crater) were able to flow down the flanks as bulldozing, thickening flows with dominantly ductile interiors and brittle exteriors; these flows collapsed as the front thickened, possibly due to a decrease in gradient, producing widespread block and ash flows. The removal of lava associated with collapse generated a decompression event which resulted in fragmentation, cracking and vesiculation in the hot interior of the lava flows. These events left behind a re-vesiculated and bread-crusting lava flow front and produced block and ash flows with abundant breadcrust bombs that reached the base of Tarawera.

**Keywords** Lava dome · Dome structure · Block and ash flow · Dome collapse

---

Editorial responsibility: J. Fierstein

---

✉ P. A. Ashwell  
paul.ashwell@canterbury.ac.nz

<sup>1</sup> Department of Geological Sciences, University of Canterbury,  
Private Bag 4800, Christchurch 8140, New Zealand

<sup>2</sup> University of Geneva, Geneva, Switzerland

## Introduction

The style of extrusion of lava domes spans a continuum between two end member styles—endogenous (inflation of a lava dome) and exogenous (extrusion of a series of lava spines or flows; Anderson and Fink 1989; Swanson et al. 1989; Fink et al. 1990; Fink and Anderson 2000; Calder et al. 2015). Many domes show a transition from one style to another due to a change in various eruption parameters such as effusion rate (Nakada et al. 1995; Calder et al. 2002;

Kaneko et al. 2002; Watts et al. 2002b), vesicularity (Platz et al. 2007; Bull et al. 2012), viscosity (Platz et al. 2007) or the development of shear zones inside the dome (Hale and Wadge 2008). Exogenous growth is associated with high viscosity, confined domes with a low effusion rate, such as Mt. St. Helens (Vallance et al. 2008), while endogenous growth accompanies unconfined domes of lower viscosity (Nakada et al. 1995) or higher effusion rates (Hale and Wadge 2008), although endogenous growth can also occur at low effusion rates (Nakada et al. 1999; Latutrie et al. 2017). The style of extrusion of a lava dome will dictate the arrangement of internal structures such as flow bands, shear zones, fractures/faults and breccia zones as well as variations in porosity, and vice versa. The textures that define different lava dome extrusions develop from both ductile and brittle deformation.

The creation and destruction of a bubble or fracture network in viscous magma controls the ability of a magma to degas effectively. Porosity in lavas can vary from 80% (in magmatic foams) to less than 10% (in dense obsidian flows, e.g. Jaupart and Allegre 1991; Klug and Cashman 1996; Castro and Cashman 1999; Mueller et al. 2011). The generally low mean porosity (<40%) of lava domes (Mueller et al. 2005) has been explained from two perspectives: (1) the failure of the magma to form bubbles in the first place either due to low water contents and/or insufficient diffusion time and too high viscosity for vesiculation, with degassing driven by tuffisite veins (e.g. Castro et al. 2014), and (2) the growth and subsequent collapse of a connected bubble network (e.g. Eichelberger et al. 1986; Westrich and Eichelberger 1994; Fink et al. 1992; Gardner et al. 1999; Gardner et al. 2000; von Aulock et al. 2017). The permeable foam model (Eichelberger et al. 1986; Fink et al. 1992) predicts that effusive lava dome activity is distinct from explosive activity, due to bubble pressure being reduced to below a fragmentation threshold (e.g. Spieler et al. 2004), but more recent observations on erupting rhyolitic volcanoes have also shown that both effusive and explosive behaviour can occur simultaneously (e.g. Schipper et al. 2013; Castro et al. 2012b). At both Chaitén and Cordon Caulle volcanoes, fracture networks and tuffisite veins allowed efficient degassing of otherwise low permeability lavas and showed that effusion of lava can still be accompanied by explosive eruptions (Schipper et al. 2013; Castro et al. 2014). These observations combined with recent experiments (Ashwell et al. 2015; Kennedy et al. 2016; Heap et al. 2016; von Aulock et al. 2017) have shown that domes may be spatially heterogeneous in porosity and permeability. This spatial variation in turn drives simultaneous and distinct mechanical and eruptive behaviour, requiring complex models of outgassing to reflect this variation over time.

The viscosity and porosity of the lava determines whether strain rate in an extruding lava dome results in brittle or ductile behaviour (Dingwell 1996; Ashwell et al. 2015; Heap et al.

2016), which also controls the production of internal structures such as flow bands, fractures and breccia zones. Crystalline domes, such as Soufrière Hills and Unzen, often form well-defined shear zones that facilitate spine extrusion and degassing (Nakada et al. 1999; Watts et al. 2002a; Sahetapy-Engel and Harris 2008; Lavallée et al. 2013), while crystal poor domes more commonly form sprawling flow fields, and contain a greater variability in vesicle segregation, but generally consistent flow bands with localised folding and deformation (Fink and Pollard 1983; Fink and Manly 1987; Manley and Fink 1987; Castro and Cashman 1999; Tuffen et al. 2013).

Flow banding is a common texture in effusive lava, and is created during viscous deformation of the magma. Porosity reduction in magma occurs when bubbles compact due to overburden pressure (Ashwell et al. 2015; Quane et al. 2009). Flow bands originate from velocity differences during ascent in the conduit, resulting in shear elongated bubbles and aligned crystals (Stasiuk et al. 1996; Fink and Anderson 2000). Generally, flow banding will be parallel to the edges of the conduit during ascent or emplacement (Stasiuk et al. 1996; Tian and Shan 2011), but the orientations will continue to evolve as the lava erupts. Endogenous or exogenous flow will define the orientation of flow banding from parallel to radial respectively.

Brittle deformation is also common in lava domes, especially close to the margins of the conduit of the dome where the erupting lava is in contact with cold country rock, and occurs primarily in low vesicularity lavas (Heap et al. 2016). The extrusion of spines or plugs can lead to the development of wide breccia or narrow fault zones that allow changes in extrusion rate, degassing and eruptive style (Sparks et al. 2000; Cashman et al. 2008; Sahetapy-Engel and Harris 2008; Lavallée et al. 2013; Kendrick et al. 2012; Hornby et al. 2015). Fracturing of the magma, as well as the stick-slip motion of a rising plug of magma, can lead to the generation of microearthquakes (Voight et al. 1999; Lavallée et al. 2008; Tuffen et al. 2008; Smith et al. 2009; Kendrick et al. 2014; Lamb et al. 2015), formation of tuffisite veins (Tuffen et al. 2003; Castro et al. 2014) and the development of permeable fractures that may produce planes of weakness that lead to dome failure (Kendrick et al. 2013). These processes of flow and fracture are controlled by the temporal and spatial distribution of viscosity and strain rate variations, and hence control the spatial and temporal development of lava dome facies. The complex arrangement of structures, facies and textures in a lava dome is therefore directly linked to the style of extrusion of the dome.

Dome growth is often accompanied by failure of part of the dome, potentially leading to formation of a block and ash flow. The potential for collapse of the dome is controlled by the method of dome extrusion (i.e. endogenous vs exogenous) and dome size, and may lead to a transition to an explosive eruption phase (Nakada et al. 1999; Watts et al. 2002b; Carn et al. 2004; Platz et al. 2007; Williamson et al. 2010). Block

and ash flows tend to be formed in two ways, either by gravitational collapse of an over-steepened flow front (referred to as Merapi type), such as that experienced by lava flows at Santiaguito (Rose et al. 1976; Rose 1987), or by explosion resulting from a pressurised interior (referred to as Peléan type; Fink and Kieffer 1993). Collapse of lava domes may be caused by several mechanisms such as (1) by propagation of cracks from the surface of flows on steepened slopes (c. 30°) into the relatively lower-tensile-strength base of the flow, and subsequent gravitational collapse (Sato et al. 1992; Ui et al. 1999; Platz et al. 2012); (2) undermining of the solid core of a dome by talus apron slumping exposing the dome interior (Herd et al. 2005); (3) from bulging of carapace material by the intrusion of lava during endogenous growth (Ui et al. 1999); (4) from intense rainfall on steep, unstable flanks (e.g. Carn et al. 2004); and (5) rapid expulsion of a viscous plug within the upper conduit during periods of fluctuating eruption rates (e.g. Watts et al. 2002a; Loughlin et al. 2010). Dome collapse events at Unzen (e.g. Nakada et al. 1999), Mt. St. Helens (e.g. Vallance et al. 2008), Merapi (Carr et al. 2016) and Soufrière Hills (e.g. Calder et al. 2002; Carn et al. 2004) have suggested links between collapse events and extrusion rate. Generally, collapse events were more common (Nakada et al. 1999) or were larger (Calder et al. 2002) when extrusion rates were higher. At Santiaguito, collapse of the front of lava flows produces an expanding mixture of dense and vesicular material suggesting that lava flow failure can still access hot, pressurised material which vesiculates and partially fragments upon exposure to the atmosphere (Rose et al. 1976). Similar conclusions were drawn by Dennen et al. (2014) from block and ash flows sourced from Panum Dome, where material from both the cold brittle carapace and hot ductile interior was included in collapse episodes.

At Unzen, higher extrusion rates were linked to exogenous dome growth (Nakada et al. 1999), and coincided with the highest number of daily block and ash flows (Ui et al. 1999). These exogenous flows generated cracks on lava surfaces, liberating gas and thus reducing pore gas pressure (which is heterogeneous within the lavas; Sato et al. 1992), but also propagating into the basal, lower-tensile-strength portion of the flow (Ui et al. 1999). Here, the pore pressure exceeds the tensile strength of the lava, creating a local explosion and setting off fragmentation within the now free mass at the edge of the flow (Ui et al. 1999; Scheu et al. 2006). Pyroclastic flows from these events travelled up to several kilometres from source, and contained blocks of low to zero porosity, reflecting the source material from the dome (Yamamoto and Suto 1993; Miyabuchi 1999). A similar, if less clear, link between high extrusion rate and frequency of collapse episodes has also been described at Soufrière Hills Volcano (SHV; Calder et al. 2002). At SHV, periods of increased extrusion rate generally led to a higher number of rockfalls; however, similar rockfall frequencies were also recorded during periods of lower extrusion rates.

A clearer distinction at SHV is that at higher extrusion rates (up to 20 m<sup>3</sup> s<sup>-1</sup>; Wadge et al. 2010; Ryan et al. 2010) and with a higher dome volume, large dome collapse events are more common. This can lead to the collapse of either a large proportion of the dome (commonly up to 50%) or even all of the dome (e.g. Herd et al. 2005) due to the extrusion of large shear lobes and their subsequent failure (Watts et al. 2002a). The collapse is induced by over-steepened walls, but was followed by intense degassing which suggests that, similarly to Unzen, vesicles within the dome at SHV were under high pore pressure which may have also played a role in the collapse (Calder et al. 2002). From these two well-documented examples, both gravity and pore pressure plays a role, and the links between collapse scale and frequency are linked to extrusion rate, and therefore extrusion style. However, for lava domes that lack such detailed documentation of the extrusion history of the dome (but are surrounded by block and ash flow deposits), this link cannot be assumed.

Crystalline domes (Soufrière Hills, Unzen and Mt. St. Helens) are often dacitic to andesitic in composition, while crystal poor domes (e.g. Newberry, Inyo Domes) are rhyolitic in composition. Ruawahia strikes an interesting middle ground of being rhyolitic, but crystal rich (Ashwell et al. 2015), and so, its eruptive style cannot be accurately predicted by models for crystal rich, but dacitic, or crystal poor but rhyolitic magmas. Here, we present results of detailed field mapping of Ruawahia dome, and link internal structures, facies, textures and morphology to distinct styles of eruption and look at how this has created or prevented lava dome collapse and block and ash flow development.

## Geological setting

Ruawahia dome is located within the Okataina caldera complex in the central Taupo Volcanic Zone (TVZ), New Zealand (Fig. 1). The TVZ is an intra-arc, silicic- and andesitic-dominated rift system created by crustal thinning from the oblique subduction of the Pacific Plate beneath the Australian Plate (Cole and Lewis 1981; Cole 1990; Bibby et al. 1995; Wilson et al. 1995; Spinks et al. 2005). The main structural trend in the TVZ is NE–SW, with an offset of the rift axis along relict basement structures observed across Okataina caldera complex (Rowland and Sibson 2001; Acocella et al. 2003; Cole et al. 2010). This trend is observed in normal faulting (Rowland and Sibson 2001; Villamor et al. 2011), dyke intrusion (Nairn and Cole 1981; Nairn et al. 1998; Seebeck and Nicol 2009) and lava dome alignment (Leonard et al. 2010) which includes the NE–SW trend of lava domes of the Tarawera dome complex, of which Ruawahia dome is one.

Ruawahia is a ~1.5-km-diameter, high SiO<sub>2</sub> (~76 wt%; Leonard et al. 2002), high crystallinity (40–60% DRE; Ashwell et al. 2015) lava dome erupted during the 1314 AD



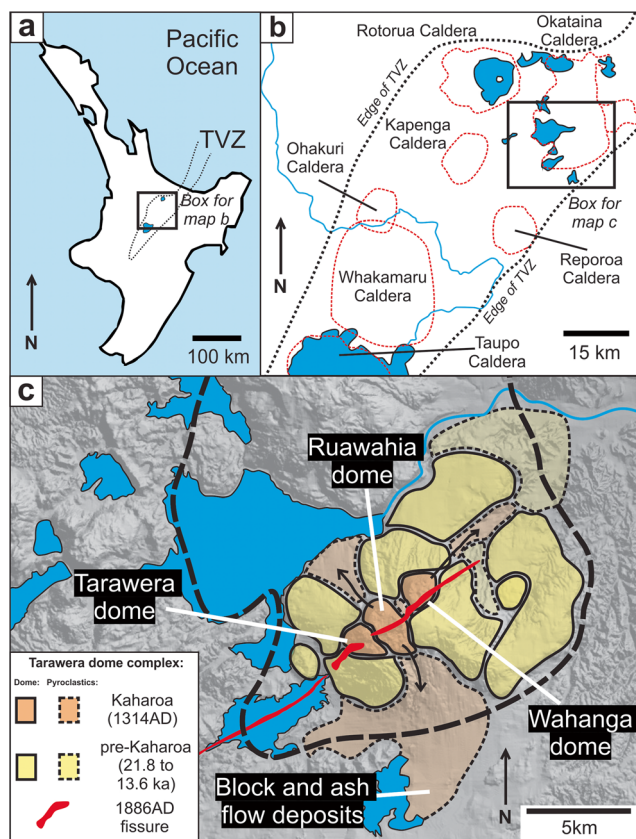


**Fig. 1** Map of location of the TVZ (a), the location of Okataina caldera within the central TVZ (b) and domes and pyroclastic deposits from the Kaharoa rhyolitic eruptions (in orange) at the Tarawera dome complex (c). Ruawahia is labelled in c

Kaharoa eruption (Cole 1970a; Nairn et al. 2001; Leonard et al. 2002; Nairn et al. 2004). The Kaharoa eruption produced three other lava domes following a Plinian eruption that built a pyroclastic cone beneath Ruawahia dome (Cole 1970b) termed Ruawahia Tuff Cone (Nairn et al. 2001). Crater Dome, to the SW of Ruawahia, was the first dome extruded, coincident with the Plinian phase, and was buried by pyroclastic material. The domes of Tarawera (SW of Crater Dome), Ruawahia and Wahanga (NE of Crater Dome) occurred following the end of explosive activity, and erupted during the same period of up to 4 years in length (Nairn et al. 2001).

Significant block and ash flow deposits occur on the NW, NE and SE slopes of the Kaharoa domes (Nairn et al. 2001) and contain sub-angular to sub-rounded blocks of varying densities in a comminuted ash matrix, all sourced from dome collapse episodes of Ruawahia and Wahanga domes, and are geochemically identical (Nairn et al. 2001). Multiple dome collapse and explosion episodes are shown by thin ash beds within the block and ash deposit in distal locations, and a mantling air-fall ash deposit on top of the block and ash flows, marking a final explosion towards the end of dome growth (Nairn et al. 2001).

Six weeks of field mapping of internal structures at Ruawahia over three field seasons was conducted on exposed

outcrops on the top and NW edge of the dome, as well as exposure within the fissure formed during the 1886 AD Tarawera eruption (Nairn and Cole 1981). During the 1886 AD Tarawera eruption, a basaltic dyke intruded through and erupted violently out of the domes (Nairn 1979; Nairn and Cole 1981; Houghton et al. 2004). The dyke re-melted the dome lava immediately adjacent to it, sealed the margins of the dyke (Kennedy et al. 2010; Schaubroth et al. 2016) and explosively excavated a series of large fissures through the cores of the lava domes, exposing the interior structures which are commonly not seen in such young lava domes.

The lava dome eruptions of Unzen, Mt. St. Helens and Soufrière Hills were extensively monitored and recorded. However, the eruption of Ruawahia in 1314 AD predates the arrival of Europeans to New Zealand (in the early 1800s), and with them a written communication system. Māori oral histories show that the first arrival of Māori to New Zealand likely coincided with the eruption of Tarawera; they are therefore the only source of information from witnesses to the eruption, and can be linked to the events recognised in the eruption sequence. Oral histories (K. Raureti, pers. comms.) inherited from the Ngāti Rangitīhi iwi (the kaitiaki, or guardians, of Tarawera) relates that the domes of the Kaharoa eruption were formed when a great chieftain, Ngātoroirangi, was called upon to battle a taniwha (a spirit), on Tarawera. Ngātoroirangi engaged and battled the taniwha (analogous to the explosive phase of the Kaharoa eruption) and was able to overcome come it; he forced it into the ground on top of Tarawera and commanded the mountain to rise up and bury the taniwha, analogous to the eruption of the Kaharoa domes towards the end of the eruption. ‘Ruawahia’ in Te Reo (the traditional Māori language) can be translated into ‘pit’ (rua-) and ‘tearing’ (-wahia) and must predate the 1886 AD eruption. This suggests that the pre-1886 AD eruption shape of the dome was one with a cleft or rift in the centre; the few accounts from before the 1886 AD eruption indicate that the overall shape of Mt. Tarawera changed very little after the eruption (Cole 1970b). However, no detailed description of the structures on the tops of the domes was completed, or have been preserved, before 1886 AD by either Māori or European sources.

## Methodology

Field mapping of Ruawahia dome was conducted over two field periods in 2011 and 2012, recording the locations of internal structures and lava dome facies, and orientations of flow bands across the dome. Samples were collected to assess porosity and petrology; thin sections were cut at the University of Canterbury using RX771c/NC epoxy resin with fluorescent green EpoDye. Porosity was measured on 25-mm-diameter and 50-mm-length cores using an ultrapycnometer 1000 with nitrogen gas.



## Descriptions of dome facies and textures

Subtle textural differences at Ruawahia were used to observe and describe three separate facies that make up the dome: (1) a core facies of porphyritic, dense, glassy to partially devitrified lava within the 1886 AD fissure and on ridges on the NW lobe (Fig. 2); (2) a carapace facies of mostly glassy pumiceous porphyritic dome rock with spherical to elongated vesicles. This facies is observed on the top and sides of the dome, and as isolated outcrops within the fissure. It includes a talus of unconsolidated blocks of lava at the edge of the dome as well as a basal breccia of angular blocks of core lava (distinguished by their low vesicularity, highly deformed bubbles and partial devitrification) within an ash-like matrix, which is located beneath the core facies (Fig. 2); (3) an interior breccia zone facies that occurs in between intact parts of the core facies with differing flow band patterns; it is only exposed in the 1886 AD fissure. The phenocrysts in all facies consist of plagioclase, quartz and rarer biotite. Flow banding in Ruawahia is generally weak, and exhibits an overall complex pattern (Fig. 2).

There is no consistent trend in dip or strike, but grouping of dip directions can be used to identify possible vent areas of individual lobes in the same area as the 1886 AD fissure.

### Core facies

The core facies consists of dense (9–33% porosity) rhyolite with variable devitrification from grey to red-brown glass with numerous spherulites to almost pristine glass. The bubbles in this facies are generally small bubbles (less than 0.5 mm) and have been highly deformed by shearing during flow (Fig. 3a). The most vesicular areas preserve elongated bubble textures with areas of microlite-rich dense glass and flat, elongated bubbles that are inter-layered with less dense, partly microlitic glass with elongated, tubular bubble structures. In heavily devitrified areas, all glass has been replaced with brown to grey spherulites and microcrystalline groundmass, crystallising preferentially along flow planes, and leaving a weak trace of the flow banding and elongate bubbles. The dense core facies is primarily found within the 1886 AD fissure, where the

**Fig. 2** Map of flow band orientations and facies distributions from outcrops on Ruawahia dome. Location of map **b** shown by red dotted box in map **a**. Stars on map **a** indicate locations of photographs in Figs. 4 and 5

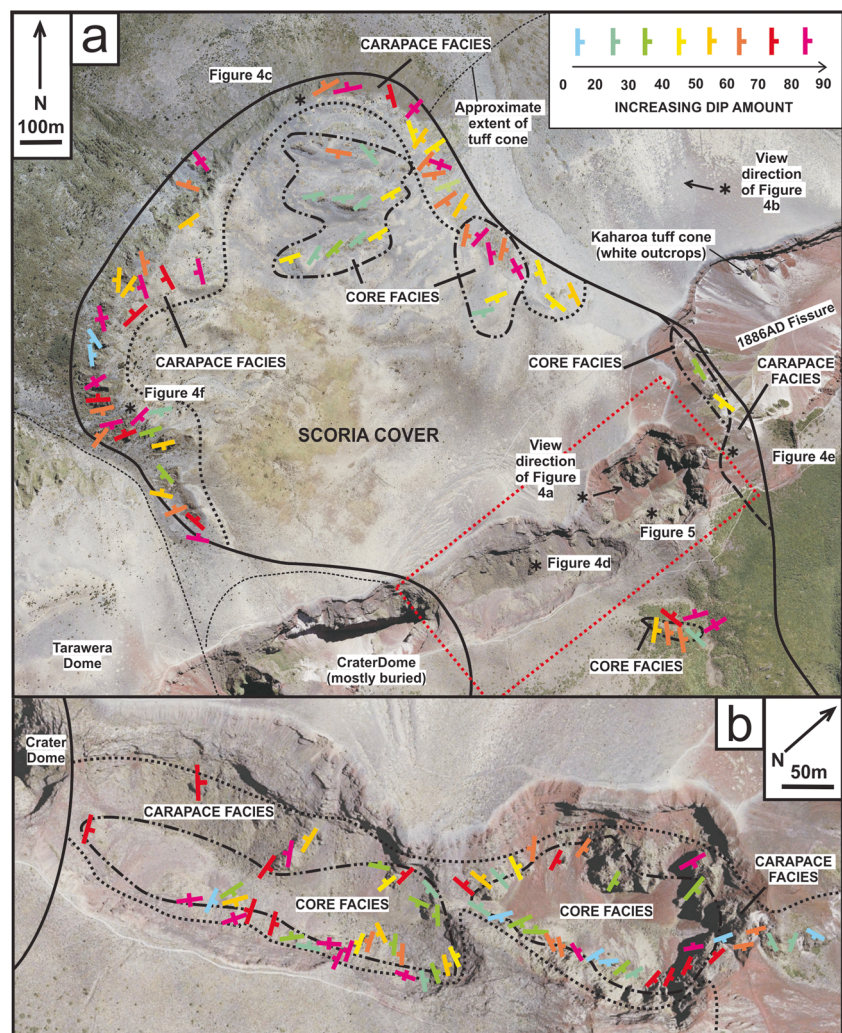
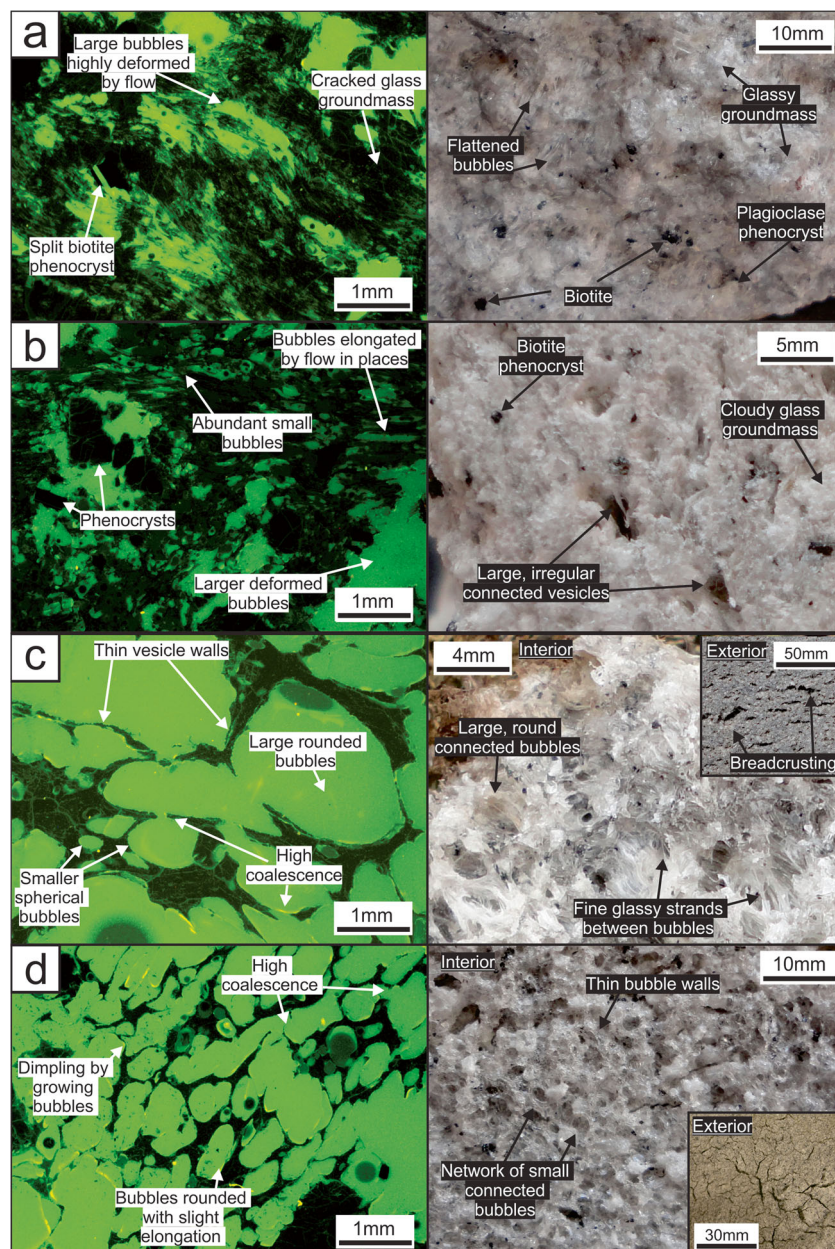




**Fig. 3** Images of thin sections (left), with a fluorescent dye (green colours indicate pore space) and hand sample photographs (right) of four bubble textures found at Ruawahia. **a** High vesicularity and spherular outcrops within the carapace facies (red outcrops in Fig. 6). **b** Typical carapace facies texture with a pumiceous appearance in outcrop (orange outcrops in Fig. 6). **c** Typical core facies textures (blue outcrops in Fig. 6). **d** Breadcrust bomb from block and ash flows to SE of Ruawahia (for comparison to **a**)



centre of the dome is exposed (Fig. 2). Here, several groupings of flow bands can be distinguished; in the north-eastern crater, a larger proportion of the flow bands dip steeply ( $> 60^\circ$ ) to the southeast (Fig. 4a). At the boundary between Crater Dome and Ruawahia dome, flow bands dip back into Ruawahia dome and intact lava is observed over-riding basal breccia. Flow banding on the north-eastern edge of Ruawahia above the pyroclastic deposits dips moderately ( $30^\circ$  to  $50^\circ$ ) back into the dome (Fig. 2). On the north-western flow lobe, a series of parallel ridges are observed where dense core facies extrudes out of the carapace facies (Fig. 4b). The ridges trend near parallel to the 1886 AD fissure. Flow banding here trends approximately parallel to the ridges and dips towards the dome summit with low to moderate dip angles (generally  $20^\circ$  to  $40^\circ$ ;

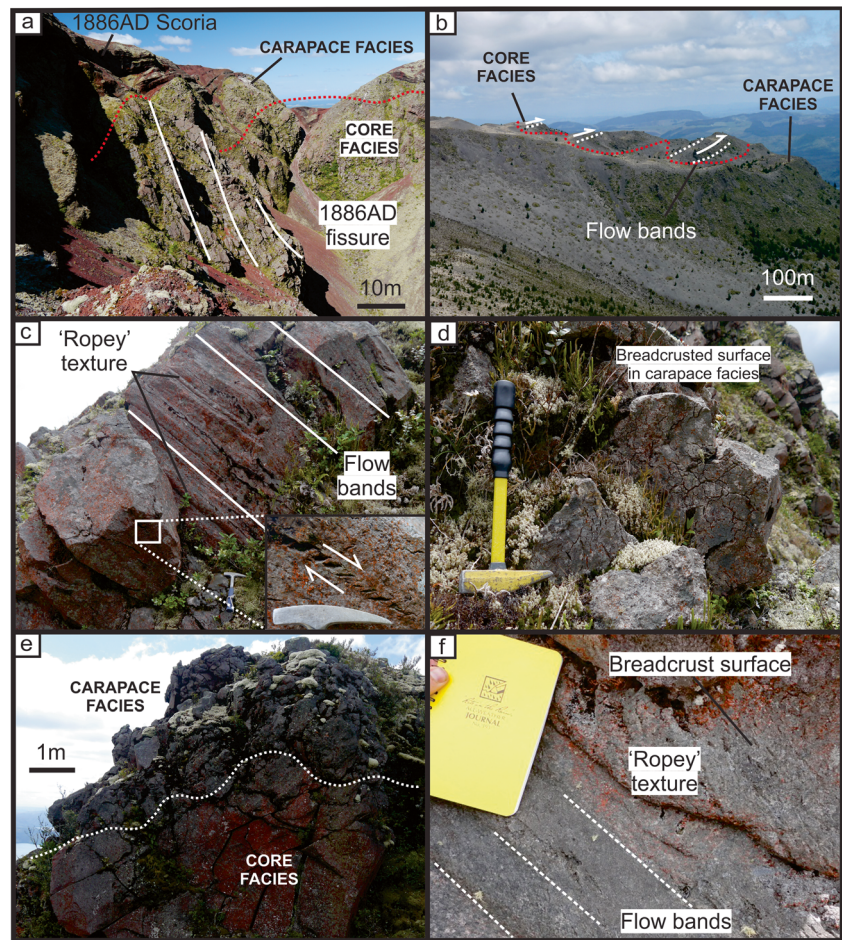
Fig. 4b). The core facies grades into the carapace facies both at the base and edges of the dome, and is most often gradational over 1 m (Fig. 4c).

### Interior breccia facies

Internal breccia facies are uncommon at Ruawahia, but they are observed between sections of differing flow band orientations within the 1886 AD fissure exposure. A 2–5-m-wide breccia zone of unconsolidated, angular rhyolite blocks in an unconsolidated matrix occurs between south-east dipping and east to north-east dipping bands (Fig. 5). Direction of movement within the breccia zone is difficult to establish as the lithology surrounding the breccia zone is highly devitrified rhyolite.



**Fig. 4** Photographs of selected outcrops at Ruawahia. **a** View of near vertical flowbands (white lines) in the 1886 AD fissure. **b** Ramp structures of core facies extruding through the carapace facies. **c** Breadcrusted surface and ropey texture at collapse scar near flow front. **d** Ropey textures and shearing in outcrops within the 1886 AD fissure. See hammer at base of outcrop for scale. **e** Breadcrusted surface within the carapace facies on NE edge of Ruawahia. **f** Transition between dense core facies and partially brecciated carapace facies at N edge of Ruawahia

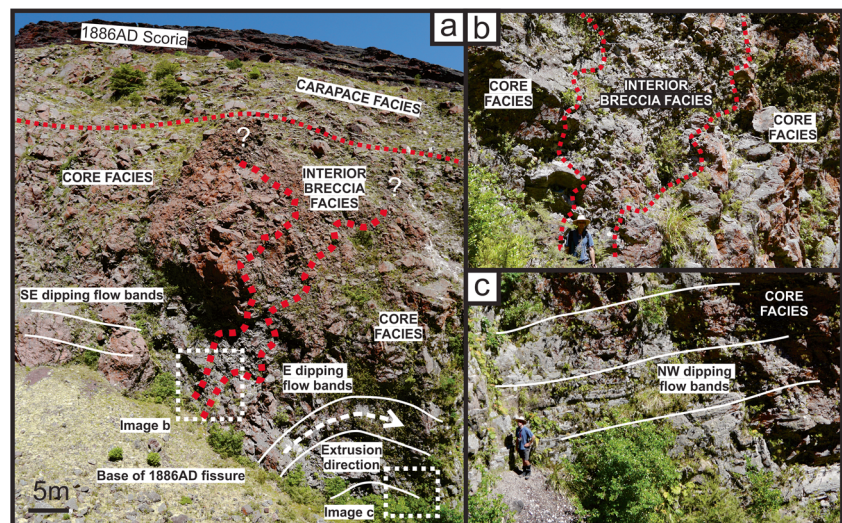


**Carapace facies**

The carapace facies has moderate to high porosity (commonly 35–70%), with elongated bubbles and a pumiceous appearance. Bubble textures in the carapace range from moderate vesicularity (less than 30%), but with small, isolated bubbles (less than

0.1 mm; Fig. 3b) to highly vesicular (up to 70%) with large, rounded, well-connected bubbles (up to 5 mm across; Fig. 3c). The majority of the carapace has a vesicularity of between 40 and 56%, with moderate to large bubbles (up to 1.5 mm) that range from irregularly shaped bubbles (often the larger bubbles) with abundant smaller and highly elongated vesicles.

**Fig. 5** Images of a breccia zone separating outcrops of lava with differing flow band orientations (**a**). Image **b** shows close-up of lower part of breccia zone, while **c** shows part of flow bands of lava forced laterally. See person for scale in **b** and **c**





The carapace facies is found along the top surface (including at the top of the 1886 AD fissure) and around the edge of Ruawahia where outcrops are not buried by 1886 AD scoria (Fig. 2). Detailed mapping of the NW edge of the dome reveals spatial variations in vesicularity and texture of outcrops, where patches of highly vesicular lava outcrop within the carapace (Fig. 6). These outcrops are extremely coarsely vesicular (62–70% porosity) pumice, with rounded vesicles (Fig. 3c) and a glassy appearance, and are observed alongside bread-crusting and ‘ropey’ textures, as well as commonly showing a non-vesicular ‘skin’ several millimetres thick; in some places, the skin is also bread-crusting (Fig. 4d). Ropey texture is a rounded skin surface that enhances the appearance of flow banding by accentuating the vesicularity differences in the bands, similar to pahoehoe-like structures described by Fink et al. (1992). The ropey texture is also observed on internal dome surfaces exposed in the 1886 AD fissure (Fig. 4e). Flow banding at outcrops on the NW edge of the lava dome are often steeply dipping ( $>70^\circ$ ) or near vertical, with strike ranging from NE–SW to N–S, in contrast to the flow banding in outcrops of the dense core facies extruding out of the top of the dome surface (e.g. Fig. 4e).

The carapace facies contains basal breccia and unconsolidated talus breccia observed at the very edge of the dome, but most of it has been buried by deposits from the 1886 AD eruption. The talus breccia in the carapace facies is observed on the north-western edge of the dome, and consists of clasts (up to 0.75 m) of vesicular lavas (occasionally with breadcrust textures) with little intra-clast matrix (Fig. 4f). The talus breccia is taken to be the large apron of material that surrounds the dome. The basal breccia is assumed to be the talus breccia

which has become over-ridden by the moving lava, as it consists of large angular blocks of dense core facies within an ash-like matrix, and grades over several metres into underlying pyroclastic material of the initial explosive phase of the Kaharoa eruption (Nairn et al. 2001).

### Block and ash flow textures

The deposits from the block and ash flows have been previously described by Nairn et al. (2001) and Hanenkamp (2011). Blocks within the block and ash flow deposits exposed by quarrying to the SE of Ruawahia (and considered to have been sourced from Ruawahia; Nairn et al. 2001) exhibit a similar range in vesicularity to that seen within the dome facies. Crucially, bread-crusting blocks within the deposit are texturally similar to the highly vesicular outcrops within the carapace (however, the maximum size of coalesced bubbles is generally smaller; Fig. 3d). These blocks also show indents where they were in contact with denser, non-bread-crusting blocks during transport and deposition.

### Facies and bubble texture interpretation

The distinct character of each facies, and their spatial distribution, at Ruawahia dome suggests a more complex extrusion pattern than the single endogenous coulée flow previously suggested by Cole (1970b). Most of the lava outcrops at Ruawahia show evidence of post-extrusion bubble closure in their low overall vesicularity (especially in the dense core) and highly irregular, deformed and occasionally isolated bubble

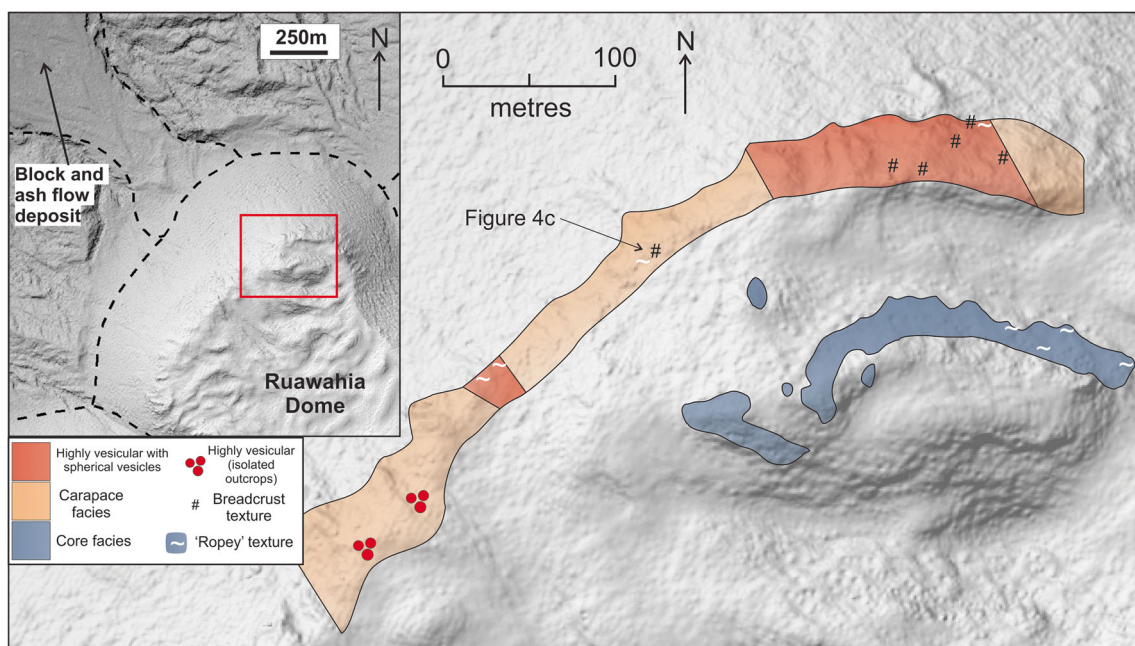


**Fig. 6** Detailed map of outcrops on NW corner of Ruawahia dome (inset shows location on dome)

shapes. The difference in vesicle size and shape between the core and carapace can be attributed to the amount of collapse or inflation of bubbles during lava dome growth, since as magma rises and extrudes, bubbles will form and grow as spheres (Westrich and Eichelberger 1994). However, strain variations in extruding magma will cause the bubbles to deform, often becoming elongate and forming a bubble network that enables outgassing and leads to bubble closure and isolation (Okumura et al. 2009; Caricchi et al. 2011). Isolated bubbles or bubble networks with low permeability can lead to over-pressurised vesicles as gas continues to exsolve; where the internal pore pressure eclipses the strength of the bubble walls, fragmentation will occur (Mueller et al. 2008). In the case of a lava dome, this fragmentation event can result from, or cause, a major dome collapse event followed by an explosive eruption from within the dome, which may or may not be followed by a continued explosive eruption phase (e.g. Ui et al. 1999; Calder et al. 2002; Druitt et al. 2002).

Bubble textures in the core of Ruawahia dome suggest significant porosity loss from a high eruptive porosity. Sheared and flattened large bubbles and split biotite phenocrysts provide evidence of bubble growth (causing biotite phenocrysts to rip apart) with subsequent flow of the lava deforming and flattening the bubbles. An initially high vesicularity is also suggested by high vesicularity pumiceous clasts in pyroclastic flows which immediately precede dome growth, as well as from highly vesicular clasts with less deformed bubbles within dome-sourced block and ash flows. The porosity of the initial eruptive foam was reduced to the density found in the core during and after extrusion by the surface tension, shear and compaction processes described by Kennedy et al. (2016), Okumura et al. (2009) and Ashwell et al. (2015). This process of porosity loss should lead to a reduction in permeability, and therefore the increased possibility of an explosive fragmentation event; however, cracking of the glass and crystals (see Fig. 3a) during compression accounts for only a minor reduction in permeability (Ashwell et al. 2015). Shear during flow leads to open degassing channels (e.g. Laumonier et al. 2011) due to coalescence of large bubbles (Okumura et al. 2009) or opening of small fractures in the glass (Kushnir et al. 2017) allowing gas escape and porosity loss. Surface tension within a permeable bubble network also works to close small pores, and smooths and reduces the size of large vesicles (Kennedy et al. 2016). Although the eruptive vesicularity of silicic lava is highly variable (e.g. Fink et al. 1992; Bull et al. 2012; Smith et al. 2001; Schipper et al. 2013), we suggest that the bubble textures of the carapace of Ruawahia best define the expected vesicularity during initial extrusion (similar to conclusions drawn by Bull et al. 2012 at Redoubt; see also Ashwell et al. 2015, and that the dense core represents the densified and deformed material in the centre of the lava dome that underwent porosity loss.

Ropy and breadcrust surfaces, more commonly seen on the dome carapace, are also exposed within the 1886 AD fissure (Fig. 4e). Breadcrust surfaces are associated with both rapid inflation and cooling, such as conditions experienced by bomb ejecta in Vulcanian eruptions (Wright et al. 2007). The breadcrust surfaces form due to cooling of the outer surface into a brittle state, while the interior continues to form and grow vesicles; the result is an expansion of a ductile interior against a near solidified exterior (von Aulock et al. 2017). Vesicles within breadcrust bombs are typically small, highly spherical and generally isolated (i.e. with a low permeability), suggesting that the bubbles grew rapidly before a sudden onset of quenching upon cooling of the entire bomb (e.g. Westrich and Eichelberger 1994; Mourtada-Bonnefoi and Laporte 2004). The typical surface cracks of bread-crusting are either formed due to expansion of the volume of the bomb due to internal vesiculation, or by shrinking of volume due to thermal contraction. Concave surfaces directly next to cracks indicate inflation; flat surfaces next to cracks infer thermal cracking (Wright et al. 2007). The 'degree' of bread-crusting of blocks and surfaces at Ruawahia is much less than those presented by Wright et al. (2007), as the size of cracks are much smaller, and the rinds are thinner. Both the breadcrust cracks of blocks within block and ash flows and cracks on outcrops surfaces of the dome are a mixture of inflation cracks and thermal cracks (also observed by Wright et al. 2007). We suggest that the significantly higher porosity, generally less sheared vesicles of bread-crusting blocks, shows that inflation of a hot pressurised interior was a prominent driving force behind the creation of this texture at Ruawahia.

The ropery surfaces (similar to those described by Fink et al. 1992) observed in outcrops on Ruawahia formed in a similar manner to the breadcrust blocks. They are formed by differential vesiculation of flow bands, caused by sudden exposure of the hot and pressurised surface after a collapse event has removed a low permeability rind or surface. The existence of these textures within the carapace of Ruawahia suggests that the dome underwent multiple collapse episodes during or shortly after growth, which exposed a hot, pressurised interior which then re-inflated beneath a skin (von Aulock et al. 2017). The presence of ropery surfaces on outcrops exposed within the 1886 AD fissure also indicates that the dome core is an amalgamation of several extrusion and collapse episodes, rather than a single, thick flow, or that the core was exposed during an explosion, and was re-buried by other extrusions.

The thin internal breccia zones within the 1886 AD fissure separate regions of differing flow band orientations. This suggests that the breccia zone represents the boundary between two separate extrusive units that were forced to extrude next to, or even through, earlier lobes (Fig. 5). The breccia zone is therefore an area of brittle deformation associated with shear movement of the lava; sense of movement across the breccia zone is difficult to determine as no movement indicators were

observed, but the flow bands suggest that a separate lava extrusion was forced laterally from a conduit sourced beneath an older, cooled and solidified lava mass (the E dipping flow bands on the right of the breccia zone observed in Fig. 5a). Similar brittle deformation has been well described on the edge of whaleback spines at Mount St. Helens (e.g. Cashman et al. 2008; Kendrick et al. 2012) and Unzen (Hornby et al. 2015) as well as at Torfajökull, Iceland (Tuffen and Dingwell 2005). In these locations, brittle deformation at the edges of the conduit allows solidified lava to rise in a stick-slip manner, creating a thin gouge layer that separates the moving lava from the conduit margin. At Ruawahia, the breccia zones are significantly thicker than the gouge zones at Mount St. Helens and Unzen; this may be due to the glassy nature of Ruawahia compared to the crystalline groundmass of the dacite domes, as thick breccia zones are also observed at Ngongotaha lava dome (Ashwell et al. 2013).

The carapace facies at Ruawahia encompasses all material which has been partially, or entirely, brecciated away from the core facies; when a dome is growing, it can be classified as solidified material (i.e. carapace) and deformable material (i.e. core; Hale 2008). Thick carapace and talus deposits are considered to be the result of endogenous dome growth (e.g. Nakada et al. 1995), while exogenous growth forms less carapace at higher extrusion rates (Griffiths and Fink 1993). The carapace of the 1981–1982 Mount St. Helens dacite dome took a few days after extrusion to fully form; the vesicular material on the flow surface becoming scoriaceous as the flow moved away from the vent (Cashman and Taggart 1983). The brecciation of the vesicular material was likely controlled by the rate of extrusion and downslope velocity (Cashman and Taggart 1983). The presence of a carapace, even as low as 2 m thick, will provide a thermal insulating layer to a lava, which may enable a flow to continue moving for considerable distances (Manly 1992). Thick carapaces (in the order of 10 m vertically, and 35 m laterally) enabled the rhyolitic flow of Cordón Caulle, Chile, to advance for ~3.6 km from the vent site, even after effusion from the vent had ceased (Tuffen et al. 2013). The relative lack of a thick carapace at Ruawahia would have resulted in a higher cooling rate which, combined with the increased viscosity due to the high phenocryst content (Ashwell et al. 2015), could account for the much smaller flow length (~1 km from the vent) but much thicker flow (~100 to 150 m), despite relatively higher topographic gradient, when compared to other lava domes.

## Flow band orientations

The orientation of flow bands at Ruawahia is complex and does not follow the predicted orientation pattern for an endogenously inflated coulée previously suggested by Cole (1970b). The orientations of flow bands around the outside

edge of the NW flow lobe are often perpendicular to the outside edge, and with high degrees of dip (generally > 70°; Fig. 2). In contrast, flow bands observed within the core facies that protrudes out of the top of the NW flow surface dip back towards the vent locations. These flow bands are interpreted to be ramp structures protruding out from the lobe as the flow front stalled (Cas and Wright 1988), similar in formation to ridges formed from compression in the Cordón Caulle lava flow observed by Farquharson et al. (2015). However, the flow bands in the outcrops along the flow edge do not match those expected from the leading edge of a flow. Instead, as part of the initial extrusives, these flow bands may have become highly deformed during the initial eruptive stage, then bulldozed at the front of the flow as more coherent lava (of the core facies) pushed the carapace ahead of it.

Flow bands within the 1886 AD fissure are also complex, but in areas (such as shown in Fig. 2b) suggest that the fissure is very close to the area of the conduit of the domes. In these areas, flow banding is near vertical and suggests that the final extrusive lavas at Ruawahia were prevented from flowing laterally and instead were forced upwards by other lava masses (in some cases forming breccia zones between them).

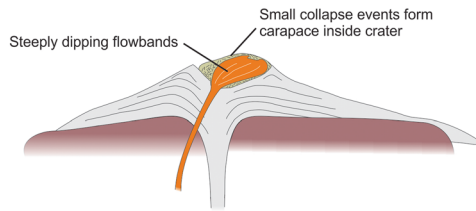
We interpret that Ruawahia formed two types of extrusives; steep spine-like lobes which were confined to the vent area either by the crater of the tuff cone formed in the initial explosive stage of the Kaharoa eruption, or by previously erupted lavas (Fig. 7a), and large flow-like lobes, which travelled down the slopes of the tuff cone (Fig. 7b). Where a spine-like lobe extruded past previous lava lobes, a breccia zone was formed due to brittle deformation; these lobes had near vertical flow bands, suggesting that they were extruded out of the conduit without much lateral movement or flow away from the vent, possibly confined by the walls of the tuff cone. Flow-like lobes either erupted outside of the crater of tuff cone, or were able to breach the wall and flow down the slopes. As the flow front cooled, it slowed and as the flow reached the base of the tuff cone with a change in topography, it stalled. Lava moving down behind the front started to bulldoze the stalled material, creating complex and often near vertical flow bands in core facies exposed at the leading edge of the flow. The core facies was eventually forced out of the surface of the flow as ramp structures (Fig. 7b); similar ramp structures were observed by Latutrie et al. (2017) at Sancy volcano, France, connected to blocks moving upwards within the lava flow in between fault zones, which were sourced to a basal shear zone enabling the near-solid mass of lava to move. No shear zone was observed at Ruawahia (due to lack of exposure of the base of the dome outside of the craters), and the deformed nature of bubbles within the core suggests that at least some deformation was taken up by the vesicles within the core.

The flow band orientations, explained by the differing types of extrusion, suggest that Ruawahia dome has erupted from multiple vents which have combined to produce the

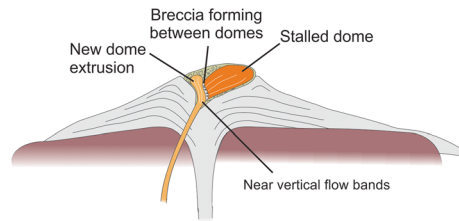


**a: Extrusion type 1: Confined - Collapse potential: Minimal***Time 1:*

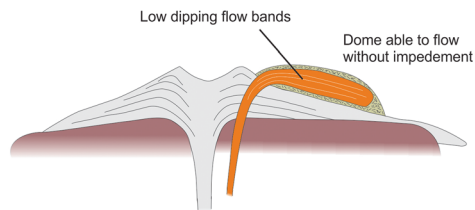
Extrusion of dome into pyroclastic cone crater; dome stalls with only small collapse events confined within crater.

*Time 2:*

Continued extrusion forces lava past stalled dome; breccia zone formed at boundary with earlier extrusion.

**b: Extrusion type 2: Unconfined - Collapse potential: High***Time 1:*

Extrusion of lobe outside of crater; able to flow downslope on flank of cone.

*Time 2:*

Dome stalls at break in slope; flow thickens and front bulldozes due to continued extrusion/ movement; collapse of flow front and vesiculation of collapse scar

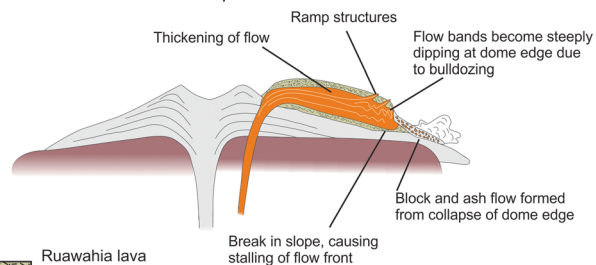


**Fig. 7** Schematic diagram of two types of dome lobe observed at Ruawahia (not to scale). Image **a** shows how a confined lobe is prevented from collapsing by the tuff cone crater, and forms breccia zones as new lobe extrusions are forced out vertically. Image **b** depicts

an unconfined flow lobe which stalls at a break in slope; continued movement of interior of dome forms ramp structures, bulldozes the front of the flow and ultimately leads to large-scale collapse

dome in its current form. These vents are likely clustered around the 1886 AD fissure; this location is where the thickest part of the dome exists, where the crater of the Kaharoa Tuff Cone is located and where the flow bands in the dome core are steepest. The exact timing of the extrusion of the confined spine-like lobes and the unconfined flow-like lobes is unclear; however, each type has a different risk of collapse and formation of block and ash flows.

## Lava dome collapse

We attribute the collapse of parts of the dome edifice at Ruawahia, and formation of widespread block and ash flow deposits, to the stalling and over-steepening of the flow front of unconfined lava, which coincides spatially to a break in topography between the base of Kaharoa Tuff Cone and underlying, older lava domes. Thin ash bands in proximal deposits suggest that the collapse of the dome was a common occurrence throughout the eruption, rather than a large single event (Nairn et al. 2001).

The deformation of the internal structures at the edge of Ruawahia occurs as the moving interior of the flow bulldozes the flow front, leading to ramp structures extruding from the interior (Fig. 7b). The over-steepened flow front is inherently

unstable (e.g. Rose et al. 1976; Calder et al. 2002), and it is likely that failure of the dome is facilitated by weaknesses within the lava, e.g. the existing shear and quench cracks (e.g. Tuffen et al. 2008; Kendrick et al. 2013; Lavallée et al. 2013) or the presence of vesicular shear bands (Okumura et al. 2009).

Textural similarities between clasts within the block and ash flow and those of Ruawahia dome show that the collapse events that formed the block and ash flow deposits were sourced from both the carapace and the core, as both vesicular and dense clasts occur within the pyroclastic deposits. The majority of clasts within the block and ash flows show no evidence of post-collapse inflation, suggesting that the majority of the material that sourced the collapse events were below the glass transition temperature. However, less common bread-crust clasts show that at least some of the block and ash flows sourced the hot and pressurised dome interior, and inflated as it was exposed to atmospheric pressure. The bubble textures within the breadcrust bombs are very similar to those observed in outcrops along the margins of lava on the NW flank of Ruawahia, and are both considerably less sheared than in the rest of the dome and the block and ash flow (Fig. 3). We interpret these high vesicularity textures to have formed during decompression without shearing due to magma movement (e.g. Gardner 2007; Castro et al. 2012a; Westrich and Eichelberger 1994). Following collapse, the hot,

pressurised interior of the dome was able to inflate considerably to form a distinctly more vesicular carapace. This volume increase may have helped to fill in scars caused by the collapse of the flow front; no obvious scars remain at the dome edge of the significant dome portion lost to form the extensive block and ash flows. Any flow of the dome after collapse would have begun to deform these bubbles, and so, we conclude that the collapse events must have occurred *in situ*, when the flow front was stationary.

The smaller bubble size of the bread-crust clasts may be attributed to a shorter cooling period before quenching; these bubbles also show a very slight elongation that is absent from highly vesicular carapace. This may be due to the expansion of already elongated bubbles (e.g. expansion of lava sourced from the flow-deformed core), or by the deformation of hot clasts within the block and ash flow itself, as the blocks often show indents where the surrounding denser blocks have prevented full inflation. High degrees of coalescence in both the breadcrust clasts and carapace outcrops suggest high permeability; this would have aided outgassing and may have prevented large-scale fragmentation of the dome (Mueller et al. 2008), even though the dome interior was pressurised during failure.

Lava which is confined to within the Kaharoa tuff cone shows a very different style of extrusion, which ultimately reduces the potential for large-scale block and ash flows (Fig. 7a). Localised ropey inflation structures present within the dome core (observed in the 1886 AD fissure; Fig. 4c) suggest that small collapse events still occurred in lavas close to the vent source. However, these locations are confined within the crater of the Kaharoa tuff cone, and therefore, the collapse events are likely to be smaller in volume, and the deposits from them confined to within the tuff cone crater. Lava extruding from vents located within the tuff cone crater are forced near vertically by the confined nature of the crater. Upon stalling of these near vertical lava lobes, continued extrusion from the vent formed a large breccia zones where newly extruded lava is forced up directly next to, or even through, previously erupted lava (Fig. 7a).

## Comparisons to other lava domes

The data we have presented here show that the main controlling factor on lava dome collapse at Ruawahia is palaeotopography; the collapse potential of the dome is higher on unconfined flow-like lobes where they meet a break in slope, and less for confined spine-like lobes. The flow-like lobes behave in a manner similar to the obsidian flows of the Inyo Dome Chain and Valles Caldera in California, USA (e.g. Manley and Fink 1987). These obsidian flows show a finely vesicular, sometimes brecciated carapace overlying dense obsidian and lithoidal rhyolite. The flow at Ruawahia shows a similar stratigraphy; however, it lacks a strongly

spherulitised core as well as layers of coarsely vesicular pumice within the dense core of the flow (Manley and Fink 1987). The lack of distinct coarse pumiceous layers in Ruawahia could be a result of the generally high vesicularity and permeability of the dome. The coarse pumice layers are thought to have occurred as a result of the trapping of volatiles beneath an impermeable layer (Manley and Fink 1987). Ashwell et al. (2015) and Kennedy et al. (2016) suggest that crystals can form a framework to enable continued outgassing in a densifying lava, thereby preventing the build-up of significant overpressure and creation of the coarsely vesicular pumice.

The limited devitrification in the core of Ruawahia could be attributed to quicker cooling rates (von Aulock et al. 2013), even though the size of Ruawahia is still comparatively large. Ridges and buckles observed by Castro et al. (2002) from the stalling of the flow front mirror the ramp structures seen at Ruawahia; the higher viscosity lava at Ruawahia (due to high crystal content) may have forced these areas to detach from the flow and extrude out as ramp structures, rather than deform as folds. The confined domes at Ruawahia behave in a way more similar to the domes of Unzen, Soufrière Hills or Mount St. Helens, creating near vertical extrusion, bounded by breccia zones. Spine growth at these examples is commonly attributed to a high effusion rate (Nakada et al. 1995), low porosity (Heap et al. 2016) or the production of a shear surface that enabled extrusion (Hale and Wadge 2008). Ruawahia did not produce true spine extrusions, but the manner in which it intruded through previously erupted lava, and formed breccia zones, is similar in concept to the ideas presented by Lavallée et al. (2012) and Kendrick et al. (2012). However, the breccia zone at Ruawahia was not as well defined as the shear zones presented by these authors, suggesting that the glassy nature of Ruawahia may result in a wider breccia zone rather than a well-defined shear zone (a feature noted by Ashwell et al. (2013) at Ngongotaha dome).

Nakada et al. (1995) suggested that the carapace of Unzen was produced inside the dome, and carried out onto the surface during extrusion, suggesting a possible link between the breccia zones and the carapace at Ruawahia. Carapace thickness is related to effusion rate; high effusion rates (and lower viscosities) form thinner carapace (Nakada et al. 1995; Griffiths and Fink 1997). The carapace over the confined lava near the 1886 AD fissure at Ruawahia is variable, but generally thicker (~20 to 40 m) than on the unconfined flow-like lobes (<10 m). Thicker carapace over the confined domes suggests that they may have had a lower effusion rate, related to forcing new lava to intrude through old domes, whereas unconfined flow-like lobes were able to move freely away from the vent and maintain relatively high effusion rates, and therefore create a thinner carapace. However, since the effusion rate of Ruawahia is unknown, we consider the confined/unconfined nature of the dome extrusions to be a primary factor in the formation of internal structures and collapse potential.

## Conclusions

The flow band textures and orientations from the dome facies at Ruawahia suggest a complex style of extrusion from multiple vents. From this evidence, as well as comparisons to the well documented eruptions at Unzen and Soufriere Hills, we highlight three new insights into characteristics and consequences of lava dome collapse:

1. Over-steepened flow front due to topography change. Many of the rockfall events at Unzen and Soufriere Hills were caused by over-steepened flow fronts due to the nature of the exogenous lava. However, at Ruawahia, we suggest that over-steepened lava forms at a change to a shallower topographic slope. The over-steepened flow front poses a great collapse hazard, with the possibility of forming large and explosive block and ash flow events.
2. Formation of highly vesicular lava with highly spherical bubble textures. Following collapse of a pressurised, and still hot, lava flow, the interior can inflate, assuming that it does not fragment. The spherical nature of the bubbles suggests in situ bubble growth. This will likely only happen in moderate (~30%) to high vesicularity, and therefore highly permeable lavas.
3. Formation of crater-confined lava domes. As new lava extrudes into a pyroclastic cone crater, brittle deformation forms breccia zones next to older, colder lava domes. If the lava is confined and unable to move laterally, then the potential for large scale collapses is much lower.

Most hazard studies on block and ash flows concentrate on the likelihood of collapse during the extrusion phase, but the hazard posed from rockfall may last for decades after the end of the extrusion (as seen by the ongoing access restrictions around Soufriere Hills; Donovan et al. 2012). This collapse hazard is increased if the dome is over-steepened (e.g. Platz et al. 2012) or affected by hydrothermal alteration during cooling (Ball et al. 2015). By recognising textures and structures that we have described here as they form, a clearer indication of collapse potential can be determined which will allow for earlier and more effective hazard management strategies for lava dome eruptions. In addition, the importance of palaeotopography and confinement of a dome in the evolution of the structures and extrusion styles show that they should be taken into account when modelling the growth and hazard potential of a lava dome.

**Acknowledgements** We would like to thank Ken Raureti and members of the Ruawahia 2B Trust for allowing access for fieldwork on Tarawera and to the two anonymous reviewers, as well as the editors J. Fierstein and A. Harris, for their insightful and thorough reviews which have greatly improved the manuscript. We wish to acknowledge the Earthquake Commission of New Zealand (EQC), Mighty River Power (MRP) and GNS Science for the primary funding for this study (part of grant 4616) as well as the Marsden Fast Start grant 09-UO-017C for providing supplementary funding.

## References

- Acocella V, Spinks KD, Cole JW, Nicol A (2003) Oblique back arc rifting of Taupo Volcanic Zone, New Zealand. *Tectonics* 22(4):1–18
- Anderson SW, Fink JH (1989) Hydrogen isotope evidence for extrusion mechanisms of the Mount St. Helens lava dome. *Nature* 341(October):521–523
- Ashwell PA, Kennedy BM, Gravley DM, von Aulock FW, Cole JW (2013) Insights into caldera and regional structures and magma body distribution from lava domes at Rotorua Caldera, New Zealand. *J Volcanol Geotherm Res* 258:187–202
- Ashwell PA, Kendrick JE, Lavallée Y, Kennedy BM, Hess K-U, von Aulock FW, Wadsworth FB, Vasseur J, Dingwell DB (2015) Permeability of compacting porous lavas. *J Geophys Res Solid Earth* 120(3):1605–1622
- Ball JL, Stauffer PH, Calder ES, Valentine GA (2015) The hydrothermal alteration of cooling lava domes. *Bull Volcanol* 77:102
- Bibby HM, Caldwell TG, Davey F, Webb T (1995) Geophysical evidence on the structure of the Taupo Volcanic Zone and its hydrothermal circulation. *J Volcanol Geotherm Res* 68(1–3):29–58
- Bull KF, Anderson SW, Diefenbach AK, Wessels RL, Henton SM (2012) Emplacement of the final lava dome of the 2009 eruption of Redoubt Volcano, Alaska. *J Volcanol Geotherm Res* 259:334–348
- Calder ES, Lockett R, Sparks RSJ, Voight B (2002) Mechanisms of lava dome instability and generation of rockfalls and pyroclastic flows at Soufriere Hills Volcano, Montserrat. *Mem Geol Soc Lond* 21:173–190
- Calder ES, Lavallée Y, Kendrick JE, Berstein B (2015) Lava dome eruptions. In: Sigurdsson H et al (eds) *Encyclopedia of Volcanoes*, 2nd edn. Academic Press, San Diego, pp 343–362
- Caricchi L, Pommier A, Pistone M, Castro JM, Burgisser A, Pergugini D (2011) Strain-induced magma degassing: insights from simple-shear experiments on bubble bearing melts. *Bull Volcanol* 73(9):1245–1257
- Carn SA, Watts RB, Thompson G, Norton GE (2004) Anatomy of a lava dome collapse: the 20 March 2000 event at Soufrière Hills Volcano, Montserrat. *J Volcanol Geotherm Res* 131(3–4):241–264
- Carr BB, Clarke AB, Vanderkluyzen L (2016) The 2006 lava dome eruption of Merapi Volcano (Indonesia); detailed analysis using MODIS TIR. *J Volcanol Geotherm Res* 311:60–71
- Cas RAF, Wright JV (1988) *Volcanic successions modern and ancient: a geological approach to processes, products and successions*. Unwin Hyman, London, p 528
- Cashman KV, Taggart JE (1983) Petrologic monitoring of 1981 and 1982 eruptive products from Mount St. Helens. *Science* 221(4618):1385–1387
- Cashman KV, Thornber CR, Pallister, JS (2008) From dome to dust: shallow crystallization and fragmentation of conduit magma during the 2004–2006 dome extrusion of Mount St. Helens, Washington. In: Sherrod DR, Scott WE, Stauffer PH (eds) *A Volcano Rekindled: The Renewed Eruption of Mt St Helens, 2004–2006*. USGS, pp 387–413
- Castro JM, Cashman KV (1999) Constraints on rheology of obsidian lavas based on mesoscopic folds. *J Struct Geol* 21:807–819
- Castro J, Cashman K, Joslin N, Olmsted B (2002) Structural origin of large gas cavities in the Big Obsidian Flow, Newberry Volcano. *J Volcanol Geotherm Res* 114:313–330
- Castro JM, Burgisser A, Schipper CI, Mancini S (2012a) Mechanisms of bubble coalescence in silicic magmas. *Bull Volcanol* 74(10):2339–2352
- Castro JM, Cordonnier B, Tuffen H, Tobin MJ, Puskar L, Martin MC, Bechtel HA (2012b) The role of melt-fracture degassing in defusing explosive rhyolite eruptions at volcán Chaitén. *Earth Planet Sci Lett* 333–334:63–69



- Castro JM, Bindeman IN, Tuffen H, Schipper CI (2014) Explosive origin of silicic lava: textural and deltaD-H<sub>2</sub>O evidence for pyroclastic degassing during rhyolite effusion. *Earth Planet Sci Lett* 405(November):52–61
- Cole JW (1970a) Petrography of the rhyolite lavas of Tarawera Volcanic Complex. *N Z J Geol Geophys* 13(4):903–924
- Cole JW (1970b) Structure and eruptive history of the Tarawera Volcanic Complex. *N Z J Geol Geophys* 13(4):881–902
- Cole JW (1990) Structural control and origin of volcanism in the Taupo volcanic zone, New Zealand. *Bull Volcanol* 52:445–459
- Cole JW, Lewis KB (1981) Evolution of the Taupo-Hikurangi subduction system. *Tectonophysics* 72:1–21
- Cole JW, Spinks KD, Deering CD, Nairn IA, Leonard GS (2010) Volcanic and structural evolution of the Okataina Volcanic Centre; dominantly silicic volcanism associated with the Taupo Rift, New Zealand. *J Volcanol Geotherm Res* 190(1–2):123–135
- Dennen RL, Bursik MI, Roche O (2014) Dome collapse mechanisms and block-and-ash flow emplacement dynamics inferred from deposit and impact mark analysis, Mono Craters, CA. *J Volcanol Geotherm Res* 276:1–9
- Dingwell DB (1996) Volcanic dilemma: flow or blow? *Science* 273(5278):1054–1055
- Donovan AR, Oppenheimer C, Bravo M (2012) Contested boundaries: delineating the “safe zone” on Montserrat. *Appl Geogr* 35(1–2):508–514
- Druitt TH, Young SR, Bapchie B, Bonadonna C, Calder ES, Clarke AB, Cole PD, Harford CL, Herd RA, Luckett R, Ryan G, Voight B (2002) Episodes of cyclic Vulcanian explosive activity with fountain collapse at Soufriere Hills Volcano, Montserrat. *Geol Soc Lond Mem* 21:281–306
- Eichelberger JC, Carrigan CR, Westrich HR, Price RH (1986) Non-explosive silicic volcanism. *Nature* 323:598–602
- Farquharson JL, James MR, Tuffen H (2015) Examining rhyolite lava flow dynamics through photo-based 3D reconstructions of the 2011–2012 lava flowfield at Cordon-Caulle, Chile. *J Volcanol Geotherm Res* 304:336–348
- Fink JH, Anderson SW (2000) Lava domes and coulees. In: Sigurdsson H et al (eds) *Encyclopedia of Volcanoes*. Academic Press, San Diego, pp 307–319
- Fink JH, Kieffer SW (1993) Estimate of pyroclastic flow velocities resulting from explosive decompression of lava domes. *Nature* 363:612–615
- Fink JH, Manley CR (1987) Origin of pumiceous and glassy textures in rhyolite flows and domes. *Spec Pap Geol Soc Am* 212:77–88
- Fink JH, Pollard DD (1983) Structural evidence for dikes beneath silicic domes, Medicine Lake Highland Volcano, California. *Geology* 11:458–461
- Fink JH, Malin MC, Anderson SW (1990) Intrusive and extrusive growth of the Mount St Helens lava dome. *Nature* 348(6300):435–437
- Fink JH, Anderson SW, Manley CR (1992) Textural constraints on effusive silicic volcanism: beyond the permeable foam model. *J Geophys Res* 97(B6):9073–9083
- Gardner JE (2007) Bubble coalescence in rhyolitic melts during decompression from high pressure. *J Volcanol Geotherm Res* 166(3–4):161–176
- Gardner JE, Hilton M, Carroll MR (1999) Experimental constraints on degassing of magma: isothermal bubble growth during continuous decompression from high pressure. *Earth Planet Sci Lett* 168:201–218
- Gardner JE, Hilton M, Carroll MR (2000) Bubble growth in highly viscous silicate melts during continuous decompression from high pressure. *Geochim Cosmochim Acta* 64(8):1473–1483
- Griffiths R, Fink J (1993) Effects of surface cooling on the spreading of lava flows and domes. *J Fluid Mech* 252:667–702
- Griffiths RW, Fink JH (1997) Solidifying Bingham extrusions: a model for the growth of silicic lava domes. *J Fluid Mech* 347:13–36
- Hale AJ (2008) Lava dome growth and evolution with an independently deformable talus. *Geophys J Int* 174(1):391–417
- Hale AJ, Wadge G (2008) The transition from endogenous to exogenous growth of lava domes with the development of shear bands. *J Volcanol Geotherm Res* 171(3–4):237–257
- Hanenkamp E (2011) Decoupling processes in block-and-ash flows: field evidence and analogue modelling. PhD thesis, University of Canterbury
- Heap MJ, Russell JK, Kennedy LA (2016) Mechanical behaviour of dacite from Mount St. Helens (USA): a link between porosity and lava dome extrusion mechanism (dome or spine)? *J Volcanol Geotherm Res* 328:159–177
- Herd RA, Edmonds M, Bass VA (2005) Catastrophic lava dome failure at Soufrière Hills Volcano, Montserrat, 12–13 July 2003. *J Volcanol Geotherm Res* 148(3–4):234–252
- Hornby AJ, Kendrick JE, Lamb OD, Hirose T, De Angelis S, von Aulock FW, Umakoshi K, Miwa T, De Angelis SH, Wadsworth FB, Hess K-U, Dingwell DB, Lavallee Y (2015) Spine growth and seismogenic faulting at Mt. Unzen, Japan. *J Geophys Res Solid Earth* 120(6):4034–4054
- Houghton BF, Wilson CJN, Del Carlo P, Coltelli M, Sable JE, Carey RJ (2004) The influence of conduit processes on changes in style of basaltic Plinian eruptions: Tarawera 1886 and Etna 122 BC. *J Volcanol Geotherm Res* 137(1–3):1–14
- Jaupart C, Allegre CJ (1991) Gas content, eruption rate and instabilities of eruption regime in silicic volcanoes. *Earth Planet Sci Lett* 102:413–429
- Kaneko T, Wooster MJ, Nakada S (2002) Exogenous and endogenous growth of the Unzen lava dome examined by satellite infrared image analysis. *J Volcanol Geotherm Res* 116(1–2):151–160
- Kendrick JE, Lavallée Y, Ferk A, Perugini D, Leonhardt R, Dingwell DB (2012) Extreme frictional processes in the volcanic conduit of Mount St. Helens (USA) during the 2004–2008 eruption. *J Struct Geol* 38:61–76
- Kendrick JE, Lavallée Y, Hess KU, Heap MJ, Gaunt HE, Meredith PG, Dingwell DB (2013) Tracking the permeable porous network during strain-dependent magmatic flow. *J Volcanol Geotherm Res* 260:117–126
- Kendrick JE, Lavallée Y, Hirose T, Di Toro G, Hornby AJ, De Angelis S, Dingwell DB (2014) Volcanic drumbeat seismicity caused by stick-slip motion and magmatic frictional melting. *Nat Geosci* 7(6):438–442
- Kennedy BM, Jellinek AM, Russell JK, Nichols ARL, Vigouroux N (2010) Time- and temperature-dependent conduit wall porosity: a key control on degassing and explosivity at Tarawera volcano, New Zealand. *Earth Planet Sci Lett* 299(1–2):126–137
- Kennedy BM, Wadsworth FB, Vasseur J, Schipper CI, Jellinek AM, von Aulock FW, Hess K-U, Russell JK, Lavallée Y, Nichols ARL, Dingwell DB (2016) Surface tension driven processes densify and retain permeability in magma and lava. *Earth Planet Sci Lett* 433:116–124
- Klug C, Cashman KV (1996) Permeability development in vesiculating magmas: implications for fragmentation. *Bull Volcanol* 58:87–100
- Kushnir ARL, Martel C, Champallier R, Arbaret L (2017) In situ confirmation of permeability development in shearing bubble-bearing melts and implications for volcanic outgassing. *Earth Planet Sci Lett* 458:315–326
- Lamb OD, De Angelis S, Umakoshi K, Hornby AJ, Kendrick JE, Lavallée Y (2015) Cyclic fracturing during spine extrusion at Unzen volcano, Japan. *Solid Earth Discuss* 7(3):2109–2149
- Latutrie B, Harris A, Médard E, Gurioli L (2017) Eruption and emplacement dynamics of a thick trachytic lava flow of the Sancy volcano (France). *Bull Volcanol* 79(4):21
- Laumonier M, Arbaret L, Burgisser A, Champallier R (2011) Porosity redistribution enhanced by strain localization in crystal-rich magmas. *Geology* 39:715–718

- Lavallée Y, Meredith PG, Dingwell DB, Hess K-U, Wassermann J, Cordonnier B, Gerik A, Kruhl JH (2008) Seismogenic lavas and explosive eruption forecasting. *Nature* 453(7194):507–510
- Lavallée Y, Mitchell TM, Heap MJ, Vasseur J, Hess K-U, Hirose T, Dingwell DB (2012) Experimental generation of volcanic pseudotachylytes: constraining rheology. *J Struct Geol* 38:222–233
- Lavallée Y, Benson PM, Heap MJ, Hess K-U, Flaws A, Schillinger B, Meredith PG, Dingwell DB (2013) Reconstructing magma failure and the degassing network of dome-building eruptions. *Geology* 41(4):515–518
- Leonard GS, Cole JW, Nairn IA, Self S (2002) Basalt triggering of the c. AD 1305 Kaharoa rhyolite eruption, Tarawera Volcanic Complex, New Zealand. *J Volcanol Geotherm Res* 115(3–4):461–486
- Leonard GS, Begg JG, Wilson CJN (2010) Geology of the Rotorua Area, Institute of Geological and Nuclear Sciences 1:250000 geological map 5. GNS Science, Lower Hutt
- Loughlin SC, Luckett R, Ryan G, Christopher T, Hards V, De Angelis S (2010) An overview of lava dome evolution, dome collapse and cyclicity at Soufriere Hills Volcano, Montserrat, 2005–2007. *Geophys Res Lett* 37(9):4–9
- Manley CR (1992) Extended cooling and viscous flow of large, hot rhyolite lavas: implications of numerical modeling results. *J Volcanol Geotherm Res* 53(1–4):27–46
- Manley CR, Fink JH (1987) Internal textures of rhyolite flows as revealed by research drilling. *Geology* 15(6):549–552
- Miyabuchi Y (1999) Deposits associated with the 1990–1995 eruption of Unzen volcano, Japan. *J Volcanol Geotherm Res* 89(1–4):139–158
- Mourtada-Bonnefoi CC, Laporte D (2004) Kinetics of bubble nucleation in a rhyolitic melt: an experimental study of the effect of ascent rate. *Earth Planet Sci Lett* 218(3–4):521–537
- Mueller SP, Melnik O, Spieler O, Scheu B, Dingwell DB (2005) Permeability and degassing of dome lavas undergoing rapid decompression: an experimental determination. *Bull Volcanol* 67(6):526–538
- Mueller S, Scheu B, Spieler O, Dingwell DB (2008) Permeability control on magma fragmentation. *Geology* 36(5):399
- Mueller SP, Scheu B, Kueppers U, Spieler O, Richard D, Dingwell DB (2011) The porosity of pyroclasts as an indicator of volcanic explosivity. *J Volcanol Geotherm Res* 203(3–4):168–174
- Nairn IA (1979) Rotomahana—Waimangu eruption, 1886: base surge and basalt magma. *N Z J Geol Geophys* 22(3):363–378
- Nairn IA, Cole JW (1981) Basalt dikes in the 1886 Tarawera rift. *N Z J Geol Geophys* 24(5–6):585–592
- Nairn IA, Kobayashi T, Nakagawa M (1998) The ~10 ka multiple vent pyroclastic eruption sequence at Tongariro Volcanic Centre, Taupo Volcanic Zone, New Zealand: part 1. Eruptive processes during regional extension. *J Volcanol Geotherm Res* 86:19–44
- Nairn IA, Self S, Cole JW, Leonard GS, Scutter C (2001) Distribution, stratigraphy and history of proximal deposits from the c. AD 1305 Kaharoa eruption of Tarawera volcano, New Zealand. *N Z J Geol Geophys* 44(3):467–484
- Nairn IA, Shane P, Cole JW, Leonard GS, Self S, Pearson N (2004) Rhyolite magma processes of the ~ AD 1315 Kaharoa eruption episode, Tarawera volcano, New Zealand. *J Volcanol Geotherm Res* 131:265–294
- Nakada S, Miyake Y, Sato H, Oshima O, Fujinawa A (1995) Endogenous growth of dacite dome at Unzen volcano (Japan), 1993 – 1994. *Geology* 23:157–160
- Nakada S, Shimizu H, Ohta K (1999) Overview of the 1990–1995 eruption at Unzen volcano. *J Volcanol Geotherm Res* 89:1–22
- Okumura S, Nakamura M, Takeuchi S, Tsuchiyama A, Nakano T, Uesugi K (2009) Magma deformation may induce non-explosive volcanism via degassing through bubble networks. *Earth Planet Sci Lett* 281(3–4):267–274
- Platz T, Cronin SJ, Cashman KV, Stewart RB, Smith IEM (2007) Transition from effusive to explosive phases in andesite eruptions—a case-study from the AD1655 eruption of Mt. Taranaki, New Zealand. *J Volcanol Geotherm Res* 161(1–2):15–34
- Platz T, Cronin SJ, Procter JN, Neall VE, Foley SF (2012) Non-explosive, dome-forming eruptions at Mt. Taranaki, New Zealand. *Geomorphology* 136(1):15–30
- Quane SL, Russell JK, Friedlander EA (2009) Time scales of compaction in volcanic systems. *Geology* 37(5):471–474
- Rose WI (1987) Volcanic activity at Santiaguito Volcano 1976–1984. *Geol Soc Am Spec Pap* 212:17–27
- Rose WI, Pearson T, Bonis S (1976) Nuee ardente eruption from the foot of a dacite lava flow, Santiaguito volcano, Guatemala. *Bull Volcanol* 40(1):23–38
- Rowland JV, Sibson RH (2001) Extensional fault kinematics within the Taupo Volcanic Zone, New Zealand: soft-linked segmentation of a continental rift system. *N Z J Geol Geophys* 44(2):271–283
- Ryan GA, Loughlin SC, James MR, Jones LD, Calder ES, Christopher T, Strutt MH, Wadge G (2010) Growth of the lava dome and extrusion rates at Soufrière Hills Volcano, Montserrat, West Indies: 2005–2008. *Geophys Res Lett* 37(19):L00E08
- Sahetapy-Engel ST, Harris AJL (2008) Thermal structure and heat loss at the summit crater of an active lava dome. *Bull Volcanol* 71(1):15–28
- Sato H, Fujii T, Nakada S (1992) Crumbling of dacite dome lava and generation of pyroclastic flows at Unzen volcano. *Nature* 360(6405):664–666
- Schauroth J, Wadsworth FB, Kennedy BM, von Aulock FW, Lavallée Y (2016) Conduit margin heating and deformation during the AD1886 basaltic plinian eruption at Tarawera volcano, New Zealand. *Bull Volcanol* 78(2):14
- Scheu B, Spieler O, Dingwell DB (2006) Dynamics of explosive volcanism at Unzen volcano: an experimental contribution. *Bull Volcanol* 69(2):175–187
- Schipper CI, Castro JM, Tuffen H, James MR, How P (2013) Shallow vent architecture during hybrid explosive–effusive activity at Cordón Caulle (Chile, 2011–12): evidence from direct observations and pyroclast textures. *J Volcanol Geotherm Res* 262:25–37
- Seebeck H, Nicol A (2009) Dike intrusion and displacement accumulation at the intersection of the Okataina Volcanic Centre and Paeroa Fault zone, Taupo Rift, New Zealand. *Tectonophysics* 475(3–4): 575–585
- Smith JV, Miyake Y, Oikawa T (2001) Interpretation of porosity in dacite lava domes as ductile-brittle failure textures. *J Volcanol Geotherm Res* 112(1–4):25–35
- Smith R, Sammonds PR, Kilburn CRJ (2009) Fracturing of volcanic systems: experimental insights into pre-eruptive conditions. *Earth Planet Sci Lett* 280(1–4):211–219
- Sparks RSJ, Murphy MD, Lejeune AM, Watts RB, Barclay J, Young SR (2000) Control on the emplacement of the andesite lava dome of the Soufriere Hills volcano, Montserrat by degassing-induced crystallization. *Terra Nova* 12(1):14–20
- Spieler O, Kennedy BM, Kueppers U, Dingwell DB, Scheu B, Taddeucci J (2004) The fragmentation threshold of pyroclastic rocks. *Earth Planet Sci Lett* 226(1–2):139–148
- Spinks KD, Acocella V, Cole JW, Bassett K (2005) Structural control of volcanism and caldera development in the transtensional Taupo Volcanic Zone, New Zealand. *J Volcanol Geotherm Res* 144(1–4): 7–22
- Stasiuk MV, Barclay J, Carroll MR, Jaupart C (1996) Degassing during magma ascent in the Mule Creek vent (USA). *Bull Volcanol* 58: 117–130
- Swanson SE, Naney MT, Westrich HR, Eichelberger JC (1989) Crystallisation history of obsidian dome, Inyo Domes, California. *Bull Volcanol* 51:161–176
- Tian Y, Shan Y (2011) The diversity of flow structures in felsic dykes. *J Geol Soc Lond* 168:1001–1011

- Tuffen H, Dingwell DB (2005) Fault textures in volcanic conduits: evidence for seismic trigger mechanisms during silicic eruptions. *Bull Volcanol* 67(4):370–387
- Tuffen H, Dingwell DB, Pinkerton H (2003) Repeated fracture and healing of silicic magma generate flow banding and earthquakes? *Geology* 31(12):1089
- Tuffen H, Smith R, Sammonds PR (2008) Evidence for seismogenic fracture of silicic magma. *Nature* 453(7194):511–514
- Tuffen H, James MR, Castro JM, Schipper CI (2013) Exceptional mobility of an advancing rhyolitic obsidian flow at Cordón Caulle volcano in Chile. *Nat Commun* 4:2709
- Ui T, Matsuwo N, Sumita M, Fujinawa A (1999) Generation of block and ash flows during the 1990–1995 eruption of Unzen Volcano, Japan. *J Volcanol Geotherm Res* 89:123–137
- Vallance JW, Schneider DJ, Schilling SP (2008) Growth of the 2004–2006 Lava-Dome Complex at Mount St. Helens, Washington. In DR Sherrod, WE Scott, PH Stauffer, eds. *A Volcano Rekindled: The Renewed Eruption of Mt St Helens, 2004–2006*. USGS Professional Paper 1750, pp 169–208
- Villamor P, Berryman KR, Nairn IA, Wilson K, Litchfield N, Ries W (2011) Associations between volcanic eruptions from Okataina volcanic center and surface rupture of nearby active faults, Taupo rift, New Zealand: insights into the nature of volcano-tectonic interactions. *Geol Soc Am Bull* 123(7–8):1383–1405
- Voight B, Sparks RSJ, Miller AD, Stewart RC, Hoblitt RP, Clarke AB, Ewart J, Aspinall WP, Baptie B, Calder ES, Cole PD, Druitt TH, Hartford C, Herd RA, Jackson P, Lejeune AM, Lockhart AB, Loughlin SC, Luckett R, Lynch L, Norton GE, Robertson R, Watson IM, Watts RB, Young SR (1999) Magma flow instability and cyclic activity at soufriere hills volcano, montserrat, british west indies. *Science* 283(5405):1138–1142
- von Aulock FW, Nichols ARL, Kennedy BM, Oze C (2013) Timescales of texture development in a cooling lava dome. *Geochim Cosmochim Acta* 114:72–80
- von Aulock FW, Kennedy BM, Maksimenko A, Wadsworth FB, Lavallée Y (2017) Outgassing from open and closed magma foams. *Front Earth Sci* 5:1–7
- Wadge G, Herd R, Ryan GA, Calder ES, Komorowski JC (2010) Lava production at Soufriere Hills Volcano, Montserrat: 1995–2009. *Geophys Res Lett* 37(3):1–6
- Watts RB, Herd RA, Sparks RSJ, Young SR (2002a) Growth patterns and emplacement of the andesitic lava dome at Soufriere Hills Volcano, Montserrat. *Geol Soc Lond Mem* 21(1):115–152
- Watts RB, Herd RA, Sparks RSJ, Young SR (2002b) The eruption of Soufriere Hills volcano, Montserrat (1995 to 1999). In: Druitt TH, Kokelaar BP (eds) *Memoirs of the Geological Society of London*. Geological Society of London, London, pp 115–152
- Westrich HR, Eichelberger JC (1994) Gas transport and bubble collapse in rhyolitic magma: an experimental approach. *Bull Volcanol* 56:447–458
- Williamson BJ, Di Muro A, Horwell CJ, Spieler O, Llewellyn EW (2010) Injection of vesicular magma into an andesitic dome at the effusive–explosive transition. *Earth Planet Sci Lett* 295(1–2):83–90
- Wilson CJN, Houghton BF, McWilliams MO, Lanphere MA, Weaver SD, Briggs RM (1995) Volcanic and structural evolution of Taupo Volcanic Zone, New Zealand: a review. *J Volcanol Geotherm Res* 68:1–28
- Wright HMN, Cashman KV, Rosi M, Cioni R (2007) Breadcrust bombs as indicators of Vulcanian eruption dynamics at Guagua Pichincha volcano, Ecuador. *Bull Volcanol* 69(3):281–300
- Yamamoto T, Suto S (1993) Pyroclastic flows from the 1991 eruption of Unzen volcano, Japan. *Bull Volcanol* 55:166–175